# Multiphase chemical engineering as a tool in modelling electromediated reactions-Example of Rh complex-mediated regeneration of NADH

Wassim El Housseini, Mathieu Etienne, Alain Walcarius, Francois Lapicque

# Multiphase chemical engineering as a tool in modelling electromediated reactions- Example of Rh complex-mediated regeneration of NADH

Wassim El Housseini[a,b], Mathieu Etienne[a], Alain Walcarius[a], Francois Lapicque[b,*]

[a] CNRS and Université de Lorraine, LCPME, UMR7564, 405 rue de Vandoeuvre, F-54600 Villers-lès-Nancy, France

[b] CNRS and Université de Lorraine, LRGP, UMR7274, ENSIC, BP 20451, F-54001 Nancy, France

**Abstract:**

On the basis of the electromediated regeneration of beta-nicotinamide adenine dinucleotide hydrate (NADH) by chloro(2,2′-bipyridyl) (pentamethylcyclopentadienyl)-rhodium (III) chloride complex – Rh(III), the manuscript describes a modelling approach inspired by multiphase chemical engineering with gas absorption with chemical reaction. Here, the electrode surface is assimilated to the gas-liquid interface, and the reducing Rh(I) formed at the electrode corresponds to the dissolved gas. This method allows the kinetics of the liquid phase reaction between $NAD^+$ and Rh(I) to be estimated and the beneficial effect of $NAD^+$ concentration on the reduction current of Rh(III) to be successfully predicted. Moreover, because of the fast kinetics of the liquid phase reaction, the overall mediated regeneration of NADH by the redox Rh couple can be viewed as occurring as the direct reduction of $NAD^+$ to NADH. The approach could be applied to other electromediated processes, upon sufficient knowledge of the system physico-chemical specificities.

**Keywords:**

Beta-nicotinamide adenine dinucleotide hydrate; chloro(2,2′-bipyridyl) (pentamethylcyclopentadienyl)-rhodium (III); electromediated reactions; gas-liquid absorption; reaction kinetics

**Correspondence:** Dr. Francois Lapicque francois.lapicque@univ-lorraine.fr

## 1- Introduction

Beta-nicotinamide adenine dinucleotide hydrate (NAD+/NADH) cofactor and its phosphorylated derivative ($NADP^+$/NADPH) are well-known electron mediators in biological systems, making it possible a number of enzymatic catalysed oxidation and reduction reactions (Steckhan, 1994; Kohlmann et al., 2008). Because of their high costs, these cofactors must be regenerated in order to enable syntheses with oxidoreductases or bio-fuel-cells applications economically viable (Kara et al., 2014; Weckbecker et al., 2010). In particular, various techniques can be used to regenerate the reducing forms NAD(P)H (Zhang et al., 2017) but electrochemical methods are often employed (Chenault et al.; 2007; Cheikhou and Tzedakis, 2008; Immanuel et al. 2020) because of their high total turnover number (TTN) allowed and no need of additional sacrificial electron donors. However, great care should be taken to produce only the bioactive 1,4-NADH and avoiding the enzymatically inactive products (such as 1,6-NADH, 1,2-NADH or NAD2 dimers) (Saba et al., 2021). The direct regeneration of NADH by reduction of $NAD^+$ at an electrode surface occurs at very cathodic potentials, thus enters in competition with hydrogen evolution and leads to the formation of the inactive dimer of $NAD^+$ (Jaegfeldt et al. 1981). For this reason, redox mediators are usually employed for this purpose (Immanuel et al., 2020; Yuan et al., 2019). These mediators can be chemical species - such as complexes of transition or precious metals cations, or organic molecules e.g. methyl viologen - biological molecules e.g. flavine adenine dinucleotide or ferredoxin $NADP^+$ reductase (FNR). All of them allow the electrochemical reduction to be conducted at less cathodic potentials and have a very high selectivity towards the regeneration of the active form of the NADH cofactor (1,4-NADH) – a crucial aspect, considering the high cycling rate of $NAD^+$/NADH in enzymatic processes.

The complex chloro(2,2′-bipyridyl) (pentamethylcyclopentadienyl)-rhodium (III) chloride was shown to be the best non-enzymatic mediator for the regiospecific regeneration of NADH (Ruppert et al., 1987; Lo et al., 1999; Holmann et al., 2003; Zhang et al., 2017) when electrochemically reduced into the monovalent rhodium (I) complex form. Using Rh(III) and Rh(I) names to relate to the two mediator forms, NADH regeneration occurs after the reaction below, with consumption of one proton per $NAD^+$ ion (which is an accepted simplified view of a multistep process, Höfer et al., 1996):

$$Rh(III) + 2\ e \rightarrow Rh(I) \qquad (1)$$

$$Rh(I) + H^+ + NAD^+ \rightarrow Rh(III) + NADH \qquad (2)$$

The principle is shown in Figure 1.

The rhodium complex can be employed as dissolved in the solution for liquid-phase reaction (2) as reported by Vuorilehto et al (2004). or in a companion paper (El Housseini et al. 2021), or grafted at the electrode surface (Tan et al. 2015; Zhang et al., 2017), for possible recycling of this expensive mediator in real bioelectrochemical processes. In both cases, $NAD^+$ reduction leads to active NADH as shown by as shown by $^1H$ NMR spectroscopy or by integration of an enzymatic reaction e.g. lactate dehydrogenase-catalysed reduction of pyruvate. Experimental measurements related to the mediated regenerations show that: (i) voltammetric curves of Rh(III) reduction exhibit far larger currents (in absolute value) in the presence of $NAD^+$ in the solution than without. (ii) batch conversion of $NAD^+$ in the presence of the Rh complex under various concentrations of the two reactants does not simply depend on one of the two concentrations. In addition, for modelling and scale-up of mediated electrochemical processes, the rate constant, k, of reaction (2) needs to be estimated.

Because of its high interest in biochemistry, the regeneration of NADH using bi-pyridines pentamethylcyclopentadienyl (cp)-rhodium complexes has been largely investigated, depending on the nature of the pyridyl functionalized groups (Steckhan et al., Lo et al., Ganesan et al.), and the nature of the Rh(III) reduction process. For this concern, the incorporation of one proton after the two electron transfers from the cathode, has often been chemically emulated by use of hydride donors e.g. sodium formate. According most published papers dealing with reduction with formate (Steckhan et al., Lo et al., Hollmann et al.), the formation rate of NADH obeys a Michaelis-Menten law involving the concentrations of Rh(III) introduced and formate ions. The low value of inhibition constant $K_M$ related to Rh(III) near 9 µM suggests that for practical applications, NADH formation rate is nearly independent of Rh(III) concentration, contrary to what has been observed with electrochemical reduction (Steckhan et al.). For both chemical and electrochemical ways to generate Rh(I) species, the rate of NADH formation is expressed in terms of turnover frequency of the Rh complex, covering the occurrences of reactions (1) and (2), with – to our state of knowledge - no quantified values for reaction rate k between Rh(I) and $NAD^+$.

In case that the redox couple is attached to the cathode surface by chemical grafting or adsorption, experimental data – in the form of voltammetric curves in motionless conditions, or under forced convection – are treated using electrochemical models developed for estimation of electrochemical and chemical kinetic parameters (Ikeda et al. 1982, Lyons et al., 1996; Lyons, 2015). When the mediating redox couple is dissolved, other interpretation

methods were developed (Wienkamp and Steckhan, 1982; Shono, 1984). Although not corresponding to mediated electrosynthesis, the case of an electrochemical process followed a chemical reaction occurring in the liquid bulk has been considered in the past (Bergel et al., 1992). Modelling of the whole system was shown to successfully benefit from previous works on gas-liquid (G-L) absorption processes with chemical reaction (Danckwerts, 1970), to calculate the enhancement of gas absorption rate by occurrence of a fast chemical reaction, as it is for the absorption of acidic $CO_2$ and $SO_2$ gases in alkaline media.

The aim of this work was to use a comparable method to model the performance of an electrochemical cell for mediated electrosynthesis - in terms of current density and conversion rate of the reactant, on the example of the above Rh/$NAD^+$ system (El Housseini et al.). In both cases, the approach relies on the existence of a diffusion layer of thickness $\delta_L$ near the (G-L or electrode-electrolyte) interface, in which transfer phenomena only occur upon diffusion, i.e. with a negligible liquid velocity (Danckwerts, 1970). For the above example of electromediated reaction, Rh(III) is named R3, Rh(I) complex, R1, whereas $NAD^+$ is referred as NAD. In the model (text and equations) for evident chemical meaning, Rh(I), Rh(III) and $NAD^+$ will still be used as such. The first step of the process is the dissolution of the gas in the liquid or the reduction of Rh(III) species on the cathode surface: in both cases, this interfacial step is assumed to be very fast. R1 formed diffuses from the cathode or reacts with NAD after (2) in the diffusion layer as shown in Figure 2.

On the basis of the above analogy, a model has been developed here for calculation of concentrations profiles in the vicinity of the electrode surface depending on the operating conditions and the rate constant k of the reaction. The limiting current density of Rh(III) reduction in the absence of $NAD^+$ allowed mass transfer coefficient of this species to be estimated. Moreover, from the experimental values for the current density at various $NAD^+$ concentrations, rate constant k could be estimated using the model. Then, progress of $NAD^+$ electromediated conversion in discontinuous tests could be simply predicted assuming a fast chemical reaction, with successful comparison to previous data for identified operating conditions.

## 2- Materials and methods

The electrochemical reactor depicted in Figure 3 was formed by two 4 x 4 $cm^2$ compartments. The anode for hydrogen oxidation into $H^+$ was a commercial gas diffusion electrode (GDE) (Ion Power) supported by a gas diffusion layer and loaded at 0.2 mg Pt/$cm^2$ was deposited on

a Nafion N-212 membrane. This membrane separated the gas/solid part of the cell from the cathode chamber for $NAD^+$ mediated reduction. The mediated reduction of $NAD^+$ was carried out on the surface of a 4 x 4 x 0.4 $m^3$ graphite felt (GFD4 6EA, SGL, Germany). The material formed from polyacrylonitrile precursor was highly porous (81%) with pores larger than 100 µm. Whereas the anode was fed with a stream of fresh hydrogen (20 $Ncm^3.min^{-1}$), the liquid phase, with a volume of 40 $cm^3$ was recirculated in the cell at 20 $cm^3.min^{-1}$ in batch NADH runs carried out at a fixed voltage and at ambient temperature. Because of the very low change in potential of the anode GDE operated with current density in the order of 1 $mA.cm^{-2}$, the cathode potential was referred to the hydrogen anode, noted ref. ($H_2$) in the manuscript. The two electrode reactions are written as:

$$Rh(III) + 2\ e^- \rightarrow Rh(I) \quad (1)$$

$$\text{with } Rh(I) + H^+ + NAD^+ \rightarrow Rh(III) + NADH \quad (2)$$

$$H_2 \rightarrow 2\ H^+ + 2\ e^- \quad (3)$$

From the above reactions, formation of one NADH molecule is accompanied by one proton gained by the solution. To avoid any visible change in the pH which has to be kept near 7, the solution contained phosphate buffer at 0.1 M.

## 3- Presentation of the model

The model was developed by analogy with G/L absorption with chemical reaction, first to predict the concentration profiles and the enhancement of the limiting current density for Rh(III) reduction by the presence of $NAD^+$. In this model, the system was assumed at steady state, on the basis of the initial concentrations of the two reactants. In contrast, time dependence was accounted for in modelling $NAD^+$ conversion in the discontinuous cell.

### 3.1. Concentration profiles near the electrode surface

For the system presented above, one-dimensional mass balances were written at steady state in the diffusion layer, thus neglecting the convective terms;

$$D_{R1}\frac{d^2C_{R1}}{dx^2} = D_{NAD}\frac{d^2C_{NAD}}{dx^2} = kC_{R1}C_{NAD} \quad (4)$$

where x is the coordinate from the electrode surface; $D_{R3}$ and $D_{NAD}$ are the diffusion coefficients of Rh(III) and $NAD^+$ in the solution, and k the rate constant of the $2^{nd}$ order kinetic law. The assumptions of the model are listed below:

- Rh(I) species was assumed to be present only in the solution even though Rh(I) was shown to be partially adsorbed on the electrode surface (Vuorilehto et al.), due to the effective solution recirculation. $NAD^+$ reduction is thus assumed to occur only in the liquid phase which justifies the expression for the kinetic term in equation (4).
- As expressed above, the electrode reduction of Rh(III) is carried out under diffusion control, so its surface concentration $C_{R3,s}$ is zero. The current density is then at its limiting value, $i_L$.
- Rh(III) and Rh(I) complexes have identical diffusion coefficients. Therefore, since Rh(III) is converted to Rh(I) with a perfect selectivity, it can be shown that:

  $$C_{R3} + C_{R1} = C_{R3,b} \text{ anywhere in the solution.} \quad (5)$$

  where subscript b refers to the solution bulk. $C_{R3,b}$ corresponds to the concentration of Rh complex introduced.
- Consumption of Rh(I) complex by the chemical reaction is assumed to be fast thus occurring only in the diffusion layer. Therefore, two boundary conditions were written:

  $x = 0$, $C_{R1} = C_{R3,b}$ and (6a)

  $x = \delta_L$, $\frac{dC_{R1}}{dx} = 0$ (6b)
- The kinetic law was written regardless of proton concentration. The presence of phosphate buffer and the pH fixed at 7.2 justify this assumption; k value holds for the pH considered.

Since $NAD^+$ is not formed or consumed at the electrode surface, its gradient at x=0 is zero; moreover, its concentration at $\delta_L$ is assumed to be that in the bulk:

$x = 0$, $\frac{dC_{NAD}}{dx} = 0$ (7a)

$x = \delta_L$, $C_{NAD} = C_{NAD,b}$ (7b)

Dimensionless length and concentrations were defined:

$$R1 = \frac{C_{R1}}{C_{R3,b}}; \quad R1 = \frac{C_{R1}}{C_{R3,b}}; \quad X = \frac{x}{\delta_L} \quad (8)$$

According to the diffusion layer film model, mass transfer coefficient $k_L$ of Rh(III) to the electrode is defined as the ratio

$$k_L = \frac{D_{R3}}{\delta_L} \quad (9)$$

Finally, Ha number was finally defined as:

$$Ha = \frac{\sqrt{kD_{R3}C_{NAD,b}}}{k_L} \quad (10)$$

Therefore, relation (4) could yield the two dimensionless differential equations:

$$\frac{d^2R1}{dX^2} = Ha^2 R1.NAD \quad (11a)$$

$$\frac{d^2NAD}{dX^2} = Ha^2 \frac{D_{R3}}{D_{NAD}} \frac{C_{R3,b}}{C_{NAD,b}} . R1.NAD \quad (11b)$$

With the boundary conditions:

$$X=0 \quad R1 = 1, \ \frac{dNAD}{dX} = 0 \quad (12a)$$

$$X=1 \quad \frac{dR1}{dX} = 0, \ NAD = 1 \quad 12b)$$

According to Danckwerts, the assumption related to a fast reaction i.e. occurring only in the diffusion layer is only valid for Ha ≥ 3, for sufficient value of rate constant k in comparison to mass transfer coefficient $k_L$, and sufficient concentration in "scavenging" $NAD^+$ species. Also introduced in G/L absorption, the enhancement factor E, defined as the ratio of the flux of Rh(III) consumption at the interface in the presence of chemical reaction to the flux without chemical reaction. In the present case, this flux is proportional to the current density, so that for mediated electrosynthesis, E is expressed as:

$$E = \frac{S_{0 with\ NAD^+}}{S_{0,without}} = \frac{i_{L,with\ NAD^+}}{i_{L,without}} \quad (13)$$

If $S_0$ is the concentration gradient of Rh(III) complex at the electrode:

$$S_0 = \frac{dR3}{dX}\Big)_{X=0} \quad (14)$$

Without occurrence of chemical reaction (no $NAD^+$ added, or k=0), the profile of Rh(III) concentration is linear, so $S_0$ is equal to -1, and relation (13) reduces to

$$E = -S_{0,without} \quad (15)$$

E is easily deduced from the voltammetric curves by dividing the current at the diffusion plateau for the considered concentration of $NAD^+$, to the corresponding recorded current without $NAD^+$. For a postulated value of k, integration of (11) has been carried out by a finite element scheme, considering the boundary conditions (12).

## 4- Results and discussion

### 4.1. Experimental results

Voltammetric curves with Rh have first been recorded at 5 mV/s between 0.2 and -0.6 V/$H_2$, in the cell containing various concentrations of Rh(III) in the 0.1 M PBS, $NAD^+$-free solution at pH 7.2. This scan rate was formerly used with this system (Zhang et al., El Housseini et al.); in other works (Steckhan et al), the scan rate was larger or equal to 9 mV/s. Although showing the increasing effect of Rh(III) concentration, together with the synergetic action of $NAD^+$ presence in the reduction current observed, the possible control of mass transfer could not be observed by a well-defined current plateau in all cases. As exemplified by Figure 4a, evidence of mass transfer control was observed near -0.25 V vs ref ($H_2$), either by a current hump peak or on the contrary by a shouldering from which the limiting current density could not be estimated with a sufficient accuracy. It was therefore preferred to proceed to four activation cycles at 5 mV/s in the above potential range, before performing a linear scan at 1 mV/s between 0 V and -0.6 V vs. $H_2$. The conversion of $NAD^+$ to NADH was estimated by the charge passed to be in the order or below 5%. Because of the above consumption of $NAD^+$ in the voltammetric experiments, each couple of Rh(III) and $NAD^+$ concentrations was investigated with a freshly prepared solution. As shown in Figures 4b and c, better-defined plateaus of Rh(III) cathodic reduction could be observed at 1 mV/s, with or without $NAD^+$ present in the solution. Replicate experiments led to deviations in the current plateau lower than 10%. Mass transfer rates of Rh(III) species could be estimated from the curves after graphical subtraction of the residual current. The limiting current with an uncertainty estimated at 10%, was shown to obey a linear function of Rh(III) concentration (Figure 5), however with a constant term. This non-zero current was attributed to a residual current $I_{res}$ not subtracted by the above procedure. The data obtained for tests with six different Rh concentrations are comprised between two linear variations with a slope respectively equal to the average slope with plus or minus 10%. The slope of the average variation led to mass transfer coefficient $k_L$, on the basis of two electrons exchanged and the area of the electrode taking as its geometrical area i.e. 16 $cm^2$ (see Appendix 1). Moreover, diffusivities $D_{R3}$ and $D_{NAD}$ have been estimated as explained in Appendix 2.

$$k_L = 4.6\ 10^{-5}\ m/s \pm 10\%,\ D_{R3} = 3.48\ 10^{-10}\ m^2/s,\ D_{NAD} = 2.4\ 10^{-10}\ m^2/s \qquad (16)$$

4.2. Concentration profiles in the diffusion layer

Calculations have been carried out for a Rhodium complex concentration of 50 µM, with 2 mM $NAD^+$, for rate constant k varying between 20 to 100 $m^3.mol^{-1}$, corresponding to Ha values ranging from 2.9 to 6.47.

For the lowest k value, Rh(I) concentration profile in the film deviates noticeably from the linear profile expected without $NAD^+$. The concentration gradient at X=0 was found near -2.83. However R1 is still near 0.06 for X=1 (Figure 6), expressing the fact that the boundary conditions do not hold perfectly: as a matter of fact, the chemical reaction although relatively fast, does not only occur in the diffusion layer. This phenomenon is less visible for k = 40 $m^3$ $mol^{-1}$ $s^{-1}$ for which gradient $S_0$ is more negative and R1 is slightly below 0.02 at X = 1: calculated concentration profiles are more reliable. For k = 100 $m^3$ $mol^{-1}$ $s^{-1}$, R1 is below 0.005 at the edge of the film (Figure 6), and the chemical reaction can be considered as "fast", i.e. occurring only in the film.

Because of its large excess in comparison to Rh complex, $NAD^+$ is little depleted in the diffusion film (Figure 6). Moreover, increasing the rate constant results – as expected - in more significant depletion of $NAD^+$ near the electrode surface.

These calculations carried out for various k values led to the corresponding values for the concentration gradients at the wall and enhancement factor E, as shown in Figure 7a below. The value for Ha number deduced from k affects strongly the enhancement factor, as shown in Figure 7b. In both figures, the curve in dotted line corresponds to Ha number below 3, i.e. for which boundary conditions related to Rh(I) conversion in the film are not fulfilled.

### 4.3. Estimation of the rate constant from electrochemical data

Residual current density $i_{res}$ evidenced in Figure 5 was assumed to be constant at 0.3 $mA/cm^2$ in all voltammetric curves, i.e. for all $NAD^+$ concentrations. In Rel (13) giving access to enhancement factor E, both limiting current densities $i_{L,without}$ and $i_{L,with\ NAD+}$ had to be corrected for current density $i_{res}$.

The experimental value for E factor was used for estimation of rate constant k: equations (11) subject to (12) were integrated: the trial and error procedure relied on the convergence of gradient $S_0$, which has to be equal to the opposite of the E value (rel. 15).

#### *4.3.1. Sensitivity analysis*

Because of the uncertainty on the limiting current in the order of 10%, sensitivity analysis of the method for k estimation was achieved on the example of 125 µM Rh complex and 2 mM $NAD^+$. In addition to the E value determined at 3.83, we considered its lower and higher estimates, within 10%. For this experiment example, the estimate for k from the "central" E value was found at 46 $m^3.mol^{-1}$, and at 35 and 58 $m^3.mol^{-1}.s^{-1}$ from the lower and higher E

values respectively. The above values show the strong sensitivity of the electrochemical technique, for which a 10% uncertainty in the limiting current recorded induces a change in k value in the order of 25%. In the three cases, R1 at the edge of the film was lower than 0.015, validating in an acceptable manner the assumption of fast reaction with complete consumption of Rh(I) in the film. The dimensionless profiles of R1 and NAD are shown in Figure 8.

*4.3.2. Determination of rate constant k*

The experimental values for the enhancement factor E estimated from CV curves for the various concentrations of $NAD^+$ and Rh complex, have been treated following the above procedure. Only experiments leading Ha number larger than 3 were shown here. Because of the uncertainties commented above, constant k was evaluated within its confidence interval:

$$k = 47 \pm 20\ m^3.mol^{-1}.s^{-1} \qquad (pH = 7.2) \qquad (17)$$

Comparison between theory and practice has been made on the basis of the enhancement factor. For each experiment treated, the predicted enhancement factor could be estimated from the profile of R1 in the film. As shown in Figure 9, the predicted E values are in accordance with their experimental values within 20%.

The expression of the Hatta number (rel. 10) clearly shows that the chemical rate constant k is subject to the value for mass transfer coefficient $k_L$. Because $k_L$ was estimated on the basis the geometrical area of the cathode, i.e. S=16 $cm^2$ as explained in the Appendix, the estimate for k is also subject to the area assumption. More precisely, k value given in rel. (17) does not have to be considered per se, but in comparison with $k_L$. On the contrary, dimensionless criterion Ha related to the kinetics of the chemical process, is determinant to examine whether this process can be considered as fast, i.e. occurring exclusively in the diffusion film or not: the various experiments carried out, clearly showed that the reaction could be constant as fast.

4.4. Simulating $NAD^+$ mediated conversion in the cell with $H_2$ anode

For these tests conducted at a fixed cathode potential corresponding to diffusion control, the solution with a volume V=40 $cm^3$ was circulated continuously in the cell. Former works dealing with G/L absorption (van Swaaij and Versteeg, 1992) often mention criterion R, which is the ratio of the maximum flow rate of $A_1$ consumption in the whole solution volume

over the maximum mole flow rate of $A_1$ generated at the interface. R can be then expressed as:

$$R = \frac{kC_{NAD,b}C_{RR3,b}V}{k_L C_{R3,b}S} = \frac{kC_{NAD,b}V}{k_L S} \quad (18)$$

where S is the geometrical area of the cathode (16 $cm^2$). Considering k = 47 $m^3\ mol^{-1}\ s^{-1}$ and $C_{NAD,b}$= 2 mM, leads to R near 2.6 $10^4$, a value expressing that the overall mediated regeneration of NADH is controlled by the rate of Rh(III) reduction. Therefore, modelling of NADH regeneration can be viewed as carried out in a batch (discontinuous) electrochemical reactor with a rate calculated regardless of the occurrence of the chemical reaction, i.e. as if $NAD^+$ reacts directly at the cathode surface. It can be observed that the nature of the rate-controlling process was the same for the median k values and for its lower and upper estimates.

The mass balance in the simplified discontinuous process carried out at the limiting current is:

$$V\frac{dC_{NAD,b}}{dt} = -\frac{I_L}{nF} = -Sk_{L,B}C_{NAD,b} \quad (19)$$

Coefficient $k_{L,B}$ in the above relation is the mass transfer coefficient for species B: because $\delta_L$ is assumed independent of the species nature in the film model, $k_{L,B}$ derives from $k_L$ (related to $A_1$) after:

$$k_{L,B} = k_L\frac{D_B}{D_A} \quad (20)$$

Integration of rel. (19) yields the usual exponential expression of the concentration expected from the above first order kinetics, from which conversion $X_{NAD+}$ of $NAD^+$ can be deduced:

$$X_{NAD+} = \frac{(C_{NAD,0}-C_{NAD})}{C_{NAD,0}} = 1 - exp\left(-\frac{Sk_{L,B}}{V}t\right) = 1 - exp(-Kt) \quad (21)$$

It can be observed that according to this simple model, the electromediated conversion of $NAD^+$ depends neither on Rh complex concentration, nor on $NAD^+$ initial concentration, thus it might be supposed that the model holds for any value of the concentration ratio $C_{NAD,0}/C_{R3,0}$. Practically, it is often considered to use concentration of Rh complex at least at a few $10^{-5}$ M for possible observation of a diffusion plateau in voltammetric curves, and $NAD^+$ concentration not larger than 10 mM.

Data reported in (El Housseini et al.) obtained with various concentrations of Rh complex and $NAD^+$ with the same initial $C_{NAD}/C_{R3}$ concentration ratio at 40 and at E = -0.5 V vs. ref.($H_2$), could be fairly well modelled by rel. (21) using the above value for mass transfer coefficient

$k_L$, without further adjustment (Figure 10). Moreover, it can be observed that the various data in the Figure correspond to a turnover frequency of Rh complex near 370 $h^{-1}$ for NADH regeneration. Because of the sufficiently fast chemical reaction between Rh(I) and $NAD^+$, regeneration of NADH can be modelled as though this species is directly reduced at the electrode surface. Additional data with $C_{NAD}/C_{R3}$ ratio at 10 only, follow the above trend, confirming the reaction mechanism. However, for ratio $C_{NAD}/C_{R3}$ at 80, NADH regeneration appears sluggisher (Figure 10) with a quite slower reaction from 20 minutes; for this ratio value, the conversion could not exceed 62% even after 120 min (data not shown). Obviously, the above simple model does not hold for such case, presumably because the mechanism of mediated electrosynthesis deviates from the simple mechanism considered here for too different concentrations of Rh complex and $NAD^+$, with possible effect of the surface reduction of $NAD^+$ by adsorbed Rh(I), a phenomenon not accounted for in the present model.

## 5- Conclusion

The present work was aimed at modelling the effectiveness of mediated electrochemical reactions conducted at fixed potential in terms of current density and conversion rates, using the approach developed in gas-liquid absorption accompanied by chemical reaction of the dissolved gas. The method relying here upon diffusion-controlled electrochemical process and applied to NADH regeneration mediated by a Rh complex, led to estimates of the rate constant of the chemical reactions between Rh(I) and $NADH^+$, in comparison to the mass transfer coefficient to the electrode surface. Moreover, because the chemical process was shown to be fast enough, i.e. occurring nearly only in the diffusion film, the electrochemical conversion of $NAD^+$ to NADH at a fixed potential can be modelled as if $NAD^+$ was directly reduced at the cathode surface. The method could be successfully applied to other electrochemical processes involving indirect reduction or oxidation, a situation often encountered in electro-organic synthesis or bioelectrochemistry.

The validity of the simple approach is nevertheless dependent on the validity of the assumptions made and related to, first diffusion-controlled electrochemical process, then fast chemical reaction between substrate B and generated $A_1$ species. In case that the reaction is not fast enough (Ha < 3), the model for the batch electrochemical process has to be modified by inserting the chemical term in the related mass balance. Moreover, care has to be taken to check the kinetic mechanism of the chemical process in the operating conditions investigated.

**Acknowledgements:** Thanks are due to CNRS for the inter-department PhD grant allocated to W. El Housseini and to contribution to the research costs.

## Appendices

1- Experimental estimation of mass transfer coefficient

This coefficient has been estimated from the limiting current for Rh(III) reduction, $I_L$, was deduced after subtraction of the residual current recorded at the same potential without Rh complex. Mass transfer coefficient was estimated considering the porous graphite felt as a flat, the very large pores of the materials allowing internal diffusion to be not controlling:

$$k_L = \frac{I_L}{nFSC_{R3}} \qquad \text{(A1)}$$

with S= 16 $cm^2$. For replicate tests for Rh complex concentration in the range 50 – 250 µM, $k_L$ was estimated at 4.6 $10^{-5}$ ± 10% $m.s^{-1}$.

2- Estimation of diffusion coefficients

Most relationships for estimation of the diffusivity of a soluble species in the solvent rely upon the molar volume of this species, $V_m$, in addition to the temperature and the molecular weight of the solvent. Molecular volumes of the two solutes have been estimated using Le Bas' incremental method (Reid et al., 1977) at 337.8 $cm^3$ $mol^{-1}$ for the Rh complex, and 588.8 $cm^3.mol^{-1}$ for $NAD^+$. For estimation of diffusivities in the aqueous solutions, the reference case of dissolved oxygen was used. Use of Wilke and Chang's relation (1955) led to estimates for diffusivities of oxygen and $NAD^+$ at least two times larger than the expected values, respectively at 1.96 $10^{-9}$ and 2.40 $10^{-10}$ $m^2.s^{-1}$ at 293 K (Aizawa et al., 1975). It was then preferred to consider the diffusivity in a solid as in the form:

$$D \sim V_m^m \qquad \text{(A2)}$$

For the molecular volume of oxygen, 25.6 $cm^3$. $mol^{-1}$, the two diffusivity values led to m near -0.67, slightly different from Wilke and Chang's value at -0.6. Finally, the diffusivity of the Rh complex was estimated from either oxygen or $NDA^+$, the two methods yielding the same value at 3.48 $10^{-10}$ $m^2.s^{-1}$.

**References**


Aizawa M., Coughlin, R.W., Charles M., 1975. Electrochemical regeneration of nicotinamide adenine dinucleotide, Biochimica Biophysica Acta 385(2), 362-375. doi:10.1016/0304-4165(75)90365-7.

Cheikhou, K., Tzedakis, T., 2008. Electrochemical microreactor for chiral syntheses using the cofactor NADH, American Institute of Chemical Engineers Journal 54(5), 1365-1376. doi: 10.1002/aic.11463.

Chenault, H.K, Whitesides, G.M, 2007. Regeneration of Nicotinamide Cofactors for use in Organic Synthesis. Applied Biochemistry Biotechnology 14(2), 147-197. doi:10.1007/BF02798431

Danckwerts P.V. 1970. Gas-Liquid reactions, McGraw-Hill, New-York.

El Housseini, W., Lapicque, F., Walcarius, A., Etienne, M., A hybrid reactor to couple $H_2$ oxidation to NADH regeneration, Electrochemical Science Advances e2100012. doi.org/10.1002/elsa.202100012

Ganesan V., Sivanesan D., Yoon S. 2017. Correlation between the structure and catalytic activity of Cp*Rh(substituted bipyridine) complexes for NADH regeneration, Inorganic Chemistry 56, 1366-1374. doi. 10.102/acs/inorggchem.6b02474.

Höfer, E., Steckhan, E., Ramos, B., Heineman, W.R., 1996. Polymer-modified electrodes with pendant $[Rh^{III}(C_5Me_5)(L)Cl]^+$-complexes formed by γ-irradiation cross-linking, Journal of Electroanalytical Chemistry 402(1-2), 115-122. doi:10.1016/0022-0728(95)04243-1.

Hollmann, F., Witholt, B., Schmid, A., 2002. $[Cp^*Rh(bpy)(H_2O)]^{2+}$: a versatile tool for efficient and non-enzymatic regeneration of nicotinamide and flavin coenzymes, Journal of Molecular Catalysis B: Enzymatic 19-20, 167-176. doi:10.1016/S1381-1177(02)00164-9.

Ikeda, T., Leidner, C.R., Murray, R.W., 1982. Kinetics of electron-transfer reactions of metal-complexes at impermeable redox active polymeric films on electrode surfaces and charge transport within the polymer film, Journal of Electroanalytical Chemistry 138, 343-365. doi: 10.1016/0022-0728(82)85087-0.

Immanuel, S., Sivasybramanian, R, Gul, R., Dar, MA., 2020. Recent progress and perspectives on electrochemical regeneration of reduced nicotinamine adenine dinucleotide, Chemistry an Asian Journal 15(24), 4256-4270. doi: 10.1002/asia.202001035.

Jaegfeldt, H. 1981. A study of the products formed in the electrochemical reduction of nicotinamide-adenine-dinucleotide, Journal of Electroanalytical Chemistry Interfacial Electrochemistry 128(C), 355-370. doi:10.1016/S0022-0728(81)80230-6.

Kara, S., Schrittwieser, J.H., Hollmann F., Ansorge-Schumacher, M.B., 2014. Recent trends and novel concepts in cofactor-dependent biotransformations, Applied Microbiology. Biotechnology 98(4), 1517-1529. doi: 10.1007/s00253-013-5441-5.

Kohlmann, C., Märkle, W., Lütz, S., 2008. Electroenzymatic Synthesis, Journal of Molecular Catalysis B: Enzymatic 51(3-4), 57-72. doi:10.1016/j.molcatb.2007.10.001.

Labrune, P., Bergel, A., 1992. Modelling of an indirect electrosynthesis process- 1 Theoretical study of the effect of dismutation of the mediator, Chemical Engineering Science 47(9), 1219-1217. doi: 10.1016/0009-2509(92)80244-7

Lo, H.C., Buriez, O., Kerr, J.B., Fish, R.H., 1999. Regioselective reduction of $NAD^+$ models with $[Cp^*Rh(bpy)H]^+$: structure-activity relationships and mechanistic aspects in the formation of the 1,4-NADH derivatives, Angewandte Chemie International Edition 38(10), 1429-1432. doi:10.1002/(SICI)1521-3773(19990517)38:10<1429::AID-ANIE1429>3.0.CO;2-Q.

Lyons, M.E.G., Greer, J.C., Fitzgerald, C.A., Bannon, T; Bartlett, P.N., 1996. Analyst 121:715-731. doi: 10.1039/an9962100715

Lyons M.E.G., 2015. The mechanism of mediated electron transfer at redox active surfaces, Electroanalysis 27, 992-1009. doi:10-1002/elan.201400640.

Reid, R.C., Prausnitz, J.M., Sherwood T.K., 1977. The properties of gases and liquids, 3rd Edition, McGraw-Hill, New-York.

Ruppert, R, Herrmann, S, Steckhan, E., 1987. Efficient indirect electrochemical in-situ regeneration of nadh:electrochemically driven enzymatic reduction of pyruvate catalyzed by d-ldh. Tetrahedron Letters 28(52), 6583-6586. doi:10.1016/S0040-4039(00)96919-3

Saba, T., Li J., Burnett, J.W.H., Howe, R.F., Kechagiopoulos, P.N., Wang, X., 2021. NADH regeneration: a case study of Pt-catalyzed $NAD^+$ reduction with $H_2$, American Chemical Society Catalysis 11(1), 283-289. doi:acscatal.0c04360.

Shono, T., 1984. Electroorganic chemistry in organic synthesis, Tetrahedron 40(5) 822-850.doi:10.1016/S0040-4020(01)91472-3.

Steckhan, E., 1994. Electroenzymatic Synthesis, Topics in Current Chemistry 170, 83-111, Springer-Verlag, Berlin Heidelberg.

Van Swaaij, W.P.M., Versteeg, G.F., 1992. Mass-transfer accompanied with complex reversible chemical reactions in has-liquid systems, Chemical Engineering Science 47(13-14), 3181-3195. doi: 10.1016/0009-2509(92)85028-A

Tan B, Hickey D.P., Milton R.D., Giroud F., Minteer S.D. 2015. Regeneration of the NADH Cofactor by a Rhodium Complex Immobilized on Multi-Walled Carbon Nanotubes, Journal of the Electrochemical Society 162(3) H102-H107. Doi: jes. 194.167.7.64

Vuorilehto K., Lutz S., Wandrey C. 2004. Indirect electrochemical reduction of nicotinamide coenzymes, Bioelectrochemistry 65, 1-7. Doi:10.1016/j.bioelechem.2004.05.006

Weckbecker, A., Gröger, H., Hummel, W., 2010. Regeneration of nicotinamide coenzymes: principles and applications for the synthesis of chiral compounds, in: Wittmann C., Krull R. (Eds) Biosystems Engineering I. Advances in Biochemical Engineering/Biotechnology, 120, 195-242, Springer, Berlin, Heidelberg. doi:10.1007/10_2009_55.

Wienkamp, R, Steckhan, E., 1982. Indirect Electrochemical Regeneration of NADH by a Bipyridinerhodium(I) Complex as Electron-Transfer Agent. Angewandte Chemie International Edition 21(10), 782-783. doi:10.1002/anie.198207822

Wilke, C.R., Chang, P., 1955. Correlations of diffusion coefficients in dilute solutions, American Institute of Chemical Engineers Journal 1, 254-270. doi:10.1002/aic.690010222.

Yuan, M., Kummer, M.J., Milton, R.D., Quah, T., Minteer, S.D., 2019. Efficient NADH regeneration by a redox polymer-immobilized enzymatic system, ACS Catalysis 9(6), 5486-5495. doi:acscatal. 9b00513.

Zhang, L, Etienne, M, Vilà, N, Walcarius, A., 2017. Functional Electrodes for Enzymatic and Microbial Bioelectrochemical Systems. In: Brun N, Flexer V. (Eds). Functional Electrodes for Enzymatic and Microbial Electrochemical Systems. World Scientific, 215-271. doi:10.1142/9781786343543_0006

**Figure captions**

Figure 1: Principle of the electromediated system investigated here, with occurrence of chemical reaction in the liquid phase.

Figure 2: Schematic view of the overall NADH regeneration mediated by Rh complex: Electrode reduction of R3 forming R1, which chemically reacts with dissolved NAD species.

Figure 3: Electrochemical cell for NADH generation with recirculation of the Rh complex - $NAD^+$ containing solution

Figure 4a) Cyclic voltammograms recorded at 5 $mV.s^{-1}$ (Scan 3) with the graphite felt electrode in the buffer solution with 125 µM $[Cp^*Rh(bpy)Cl]^+$: two replicates.

Figure 4b and c: Voltammetric curves recorded at 1 mV/s after 4 successive cycles at 5 mV/s for Rh complex solution with increasing amounts of NAD+: b) with 50 µM Rh(III), c) with 100 µM Rh(III) complexes. Experiments were carried out in 0.1 M phosphate buffer solution at pH 7.2 under nitrogen atmosphere with a solution and hydrogen flow rates of 20 $mL.min^{-1}$ each.

Figure 5: Variations of the limiting current density estimated from voltammetric curves at 1 mV/s with the Rh(III) solutions. Data are given with a 10% error bar, the liner regression is in solid lines and the two dotted lines are linear variations with a slope 10% higher or lower than the regression slope.

Figure 6: Dimensionless concentration profiles of species $A_1$ (Rh(I) complex) and B ($NAD^+$) in the diffusion film. Concentration of Rh complex and $NAD^+$ at 50 µM and 2 mM respectively. Effect of the rate constant k in $m^3.mol^{-1}.s^{-1}$.

Figure 7: Enhancement factor E corresponding to occurrence of the chemical reaction. Concentrations of Rh complex and $NAD^+$ at 50 µM and 2 mM respectively. Fig. 7a): variation of E with rate constant k; Fig. 7b: variation of E with Hatta number Ha.

Figure 8: Dimensionless concentration profiles in the diffusion film for the three estimates of the enhancement factor (± 10%). 125 µM Rh complex and 2 mM $NAD^+$; E = 3.83. k values are in $m^3.mol^{-1}.s^{-1}$.

Figure 9: Enhancement factor calculated for k=50 $m^3.mol^{-1}.s^{-1}$ versus their experimental values; dotted lines correspond to the diagonal ± 20%.

Figure 10: $NAD^+$ conversion versus time for various $NAD^+$-over Rh complex concentration ratio. Rh complex concentrations varied from 12.5 – 62.5 µM. Experimental data (some of them from El Housseini et al.) compared to the model predictions (rel. 21).

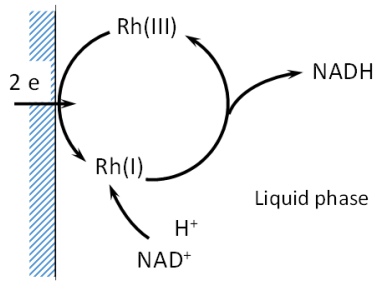


Figure 1

Figure 2

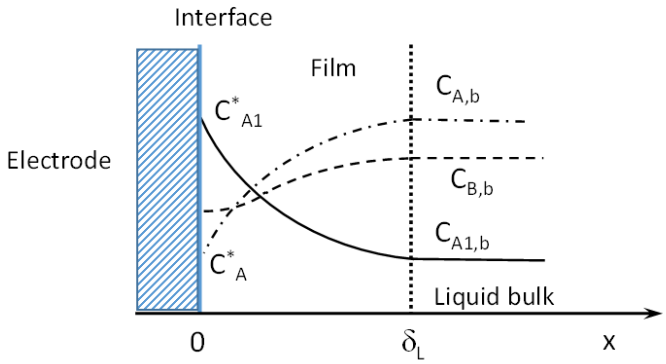


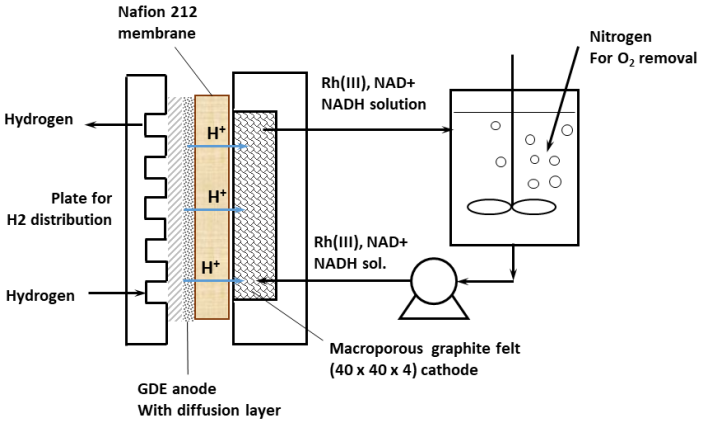

**Figure 4a**

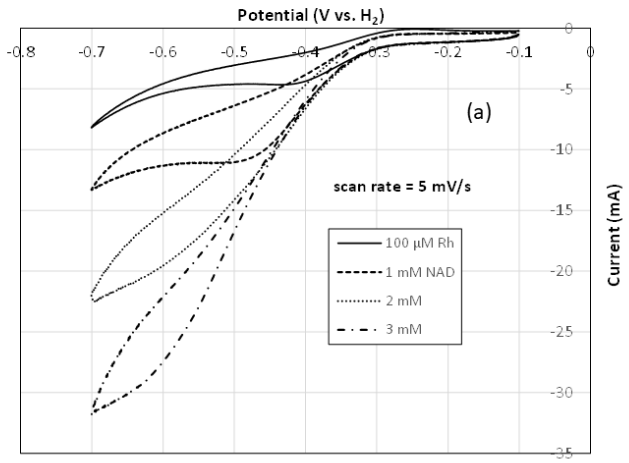


**Figure 4b and 4c**

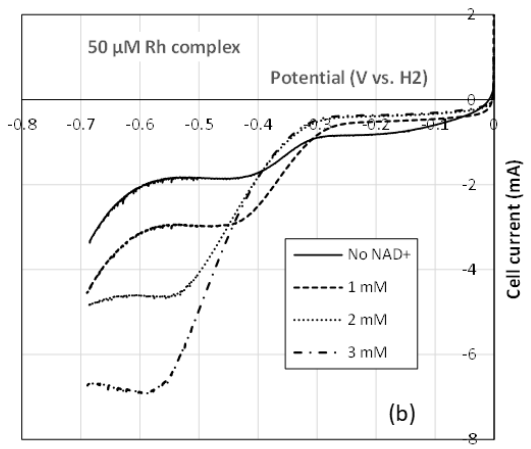


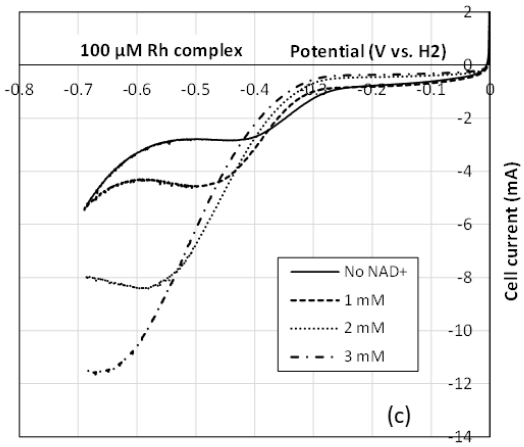


**Figure 5**

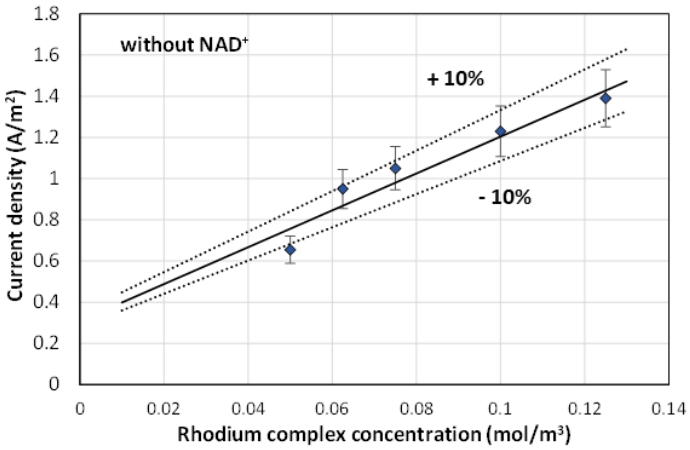

Figure 6

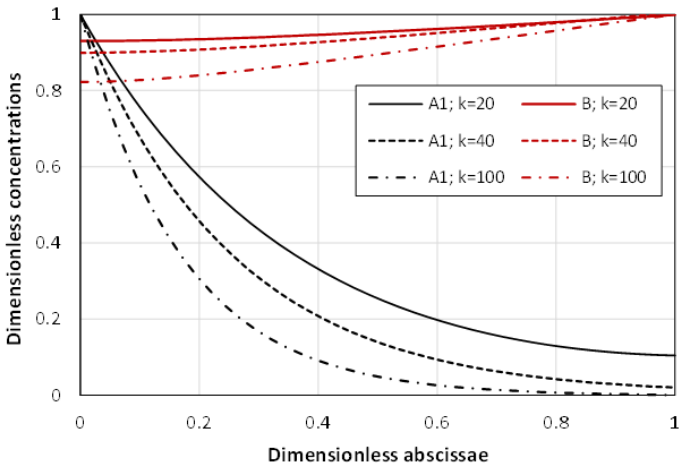


Figure 7

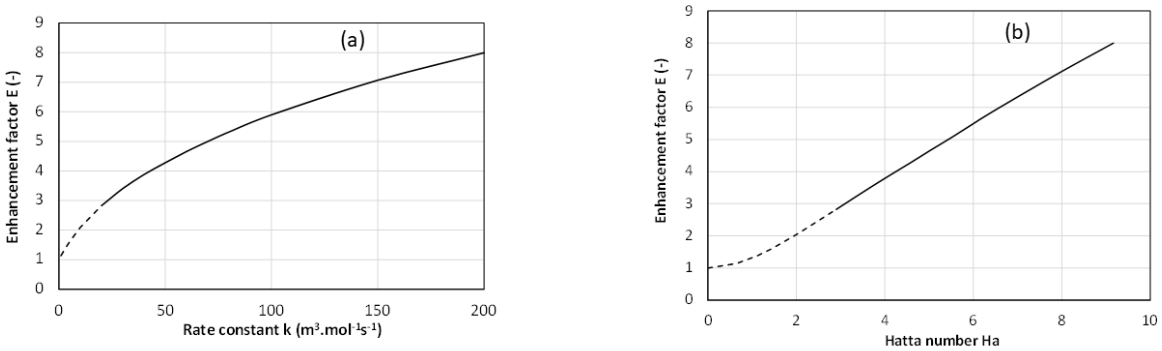


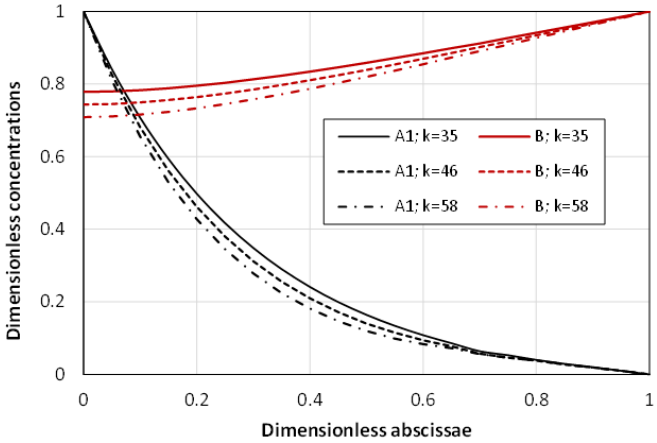


Figure 8

**Figure 9**

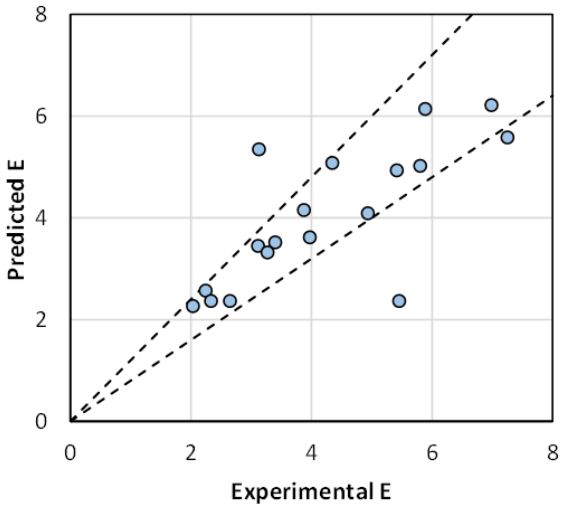


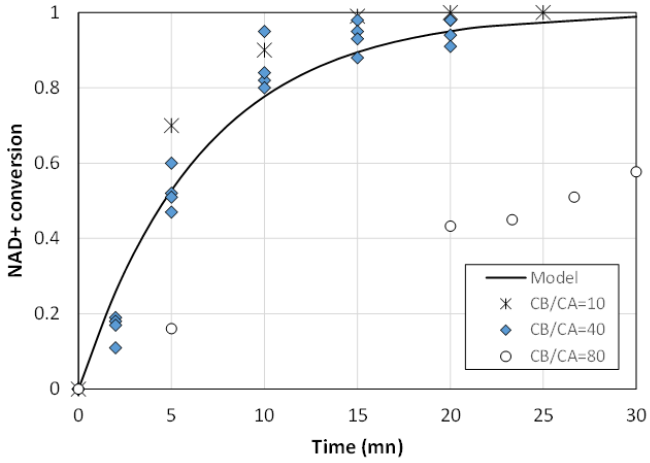


Figure 10